



## **The Current Status of Free-Flight Testing of a Scramjet-Integrated Hypersonic Cruising Vehicle Model in the Hiest Free-Piston Shock Tunnel**

*Tanno Hideyuki<sup>1</sup>, Yatsuyanagi Shuto<sup>2</sup>, Tani Kouichiro<sup>3</sup> and Tomioka Sadatake<sup>4</sup>*

### **Abstract**

A series of combustion tests were conducted in the free-piston shock tunnel Hiest in hypersonic free-stream using a 1.1-meter-long integrated scramjet airframe model, NAMaSU (New Airframe integrated Model with a Scramjet Unit). The NAMaSU is a wall-compression scramjet/airframe integrated model with a so-called lifting body concept, in which the scramjet is installed under the airframe. It is made entirely of aluminum alloy (A7075), is 1067 mm long and 224 mm wide, and weighs 37.8 kg, including all onboard equipment. The model is equipped with an internal gas-hydrogen fuel tank, a quick-acting solenoid valve, batteries, control timers, sensor and data recorders, enabling full autonomous operation as soon as the test starts. For fuel injection, the quick-acting valve was opened by a control timer triggered by a deactivation signal for the electric-magnets model holder, and gas hydrogen of up to 7 MPa was supplied from a 600 mL capacity gas-hydrogen fuel tank to the injection manifold and injected vertically into the combustor through four injection holes of  $\Phi 2$  mm orifice diameter. The aerodynamic coefficients of the three components (drag, lift, and pitching moment) were measured using the free-flight aerodynamic measurement method. The model was in free flight during the test and was aerodynamically completely non-interfering in the Hiest hypersonic free stream. The model was designed with the inlet and combustor with flight equivalent Mach number 11 conditions as nominal operating conditions. In this test series, tests were conducted on equivalent flights Mach number 9 and Mach number 11. In the tests, the hydrogen equivalent ratio was set to 1.1 by fixing the gas hydrogen tank's initial pressure, and comparative tests with and without combustion were carried out using air and pure nitrogen as test gases to extract the effect of combustion by hydrogen gas. In both the equivalent flight Mach number 9 and Mach number 11 conditions, a large pressure increase due to hydrogen combustion was observed in the combustor. Still, the measured thrust did not reach a level equivalent to the drag force of the entire model.

**Keywords :** *Hypersonic, Scramjet, Free-flight, shock tunnel*

## **1. Introduction**

### **1.1. Hypersonic scramjet**

For a hypersonic cruise vehicle equipped with a scramjet, it is essential to comprehensively evaluate the scramjet's aerodynamic stability and operating characteristics because of the strong relationship

---

<sup>1</sup>Senior Researcher, JAXA, Directorate Research and Development, 1-Koganesawa Kimigaya Kakuda Miyagi 981-1525 [tanno.hideyuki@jaxa.jp](mailto:tanno.hideyuki@jaxa.jp)

<sup>2</sup>Researcher, JAXA, Directorate Research and Development, 1-Koganesawa Kimigaya Kakuda Miyagi 981-1525 [yatsuyanagi.shuto@jaxa.jp](mailto:yatsuyanagi.shuto@jaxa.jp)

<sup>3</sup>Director, JAXA, Kakuda Research Center, 1-Koganesawa Kimigaya Kakuda Miyagi 981-1525 [tani.kouichiro@jaxa.jp](mailto:tani.kouichiro@jaxa.jp)

<sup>4</sup>Senior Researcher, JAXA, Directorate Research and Development, 1-Koganesawa Kimigaya Kakuda Miyagi 981-1525 [tomioka.sadatake@jaxa.jp](mailto:tomioka.sadatake@jaxa.jp)

between the airframe attitude and the scramjet's operating characteristics. In particular, longitudinal characteristics, or pitching moment characteristics, are critical to scramjet characteristics because the angle of attack in flight directly affects the scramjet's combustor inlet temperature and pressure.

Ground testing of scramjets at Mach 8 and above has been conducted exclusively in shock tunnels [1-7]. High stagnation point pressure and stagnation point temperature conditions, equivalent to actual flight conditions, are essential to generate a hypersonic free stream for scramjet testing, and the shock tunnels are relatively easy to achieve compared to conventional hypersonic wind tunnels. This advantage also means that high Reynolds numbers can be generated sufficient for actual flight conditions. In addition, although the test duration is short (a few milliseconds or shorter), these facilities can produce a clean test flow free of combustion products and other contaminants.

JAXA has previously conducted free-flight tests of the MoDKI (Model of Demonstrator Kakuda Initiative) [8], a 1.1-m-long integrated scramjet airframe model, in the high-enthalpy shock tunnel HIEST [9-10] to determine the three three-component aerodynamic coefficients (drag, lift, and pitching moment). The MoDKI is an all-in-one scramjet vehicle model with a gaseous fuel injection system, including a quick-acting solenoid valve, a high-pressure hydrogen tank, onboard data recorders, sensors, timers, and batteries inside the model. It was capable of fully autonomous flight tests at HIEST. However, the small size of the model meant that there was not enough space inside the model, making it difficult to outfit it with various equipment. Therefore, the combustion test in the free stream of HIEST was unsuccessful because the quick-acting solenoid valve, fuel tank, and fuel gas piping were extremely difficult to place, and the supply of gaseous hydrogen necessary for combustion was inadequate.

Therefore, based on the design knowledge obtained from the MoDKI test, a new airframe-integrated model with a Scramjet Unit (NAMaSU) was designed and built. The NAMaSU was designed to be twice as wide as the MoDKI to increase the volume inside the model and the hydrogen supply required for combustion. This report presents preliminary results of free-flight shock tunnel tests of the hydrogen gas-fueled NAMaSU at flight equivalent Mach numbers 11 and 9 in the high-enthalpy shock tunnel HIEST.

## **2. Airframe integrated scramjet vehicle model NAMaSU**

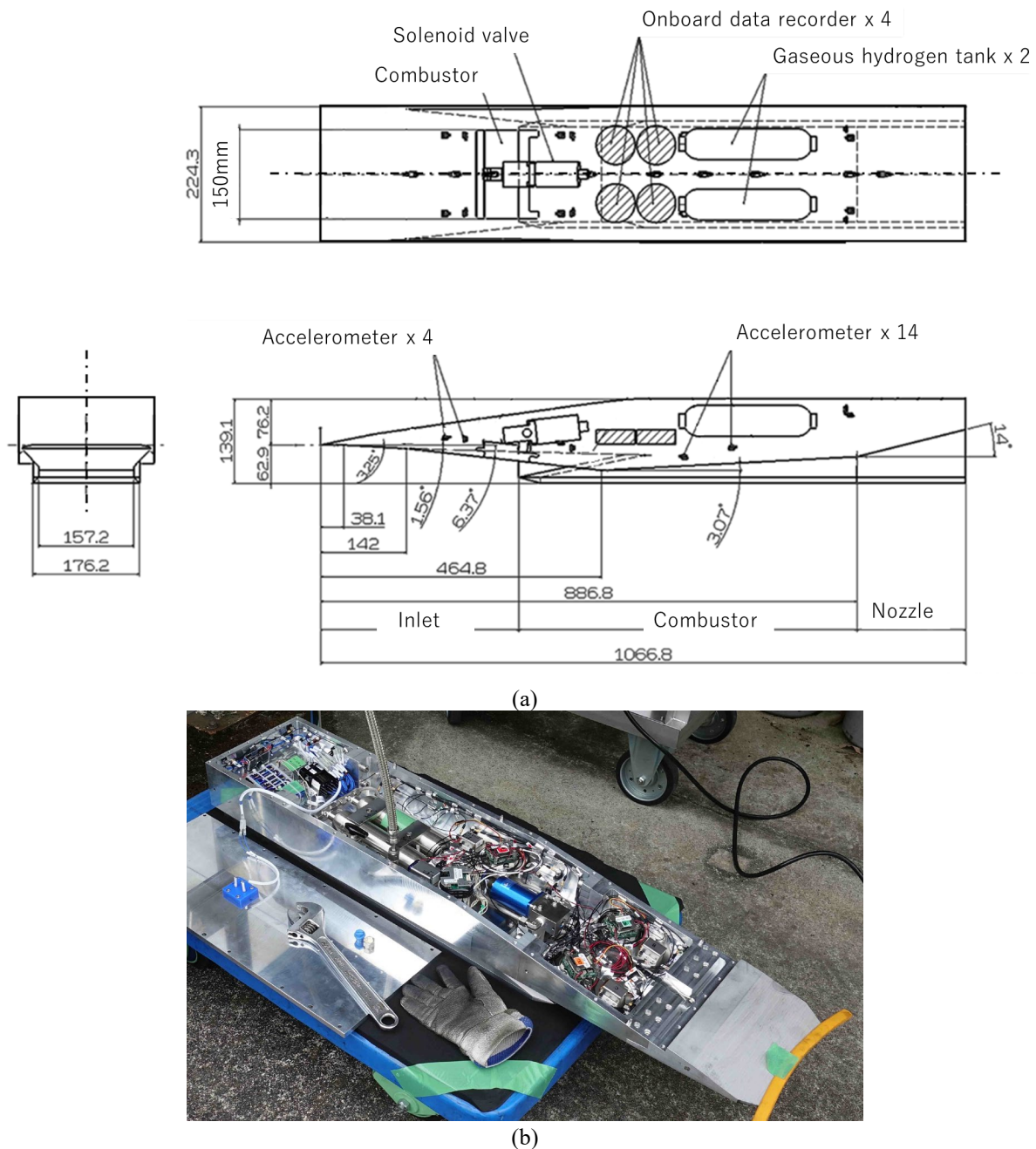
### **2.1. NAMaSU**

Figure 1 shows a schematic of the NAMaSU. By increasing the model width to twice that of the MoDKI, the internal volume of the model was significantly increased, and gas-hydrogen tanks (300 mL) were added. In conjunction with this change, the gas-hydrogen high-speed rapid open/close valve was enlarged, the fuel supply piping was expanded (from 1/4" to 1/2"), and the elbow in the supply piping was omitted as much as possible to minimize pressure loss. Gas hydrogen fuel is injected vertically into the combustion chamber. Four injection orifices are provided with an orifice diameter of 2 mm. The injection pressure of the gaseous hydrogen is measured by a piezoelectric pressure transducer (PCB113B24) attached to the manifold upstream of the injection orifice. A piezoelectric pressure transducer (PCB113B12) was used to measure the wall pressure inside the scramjet. The larger internal volume of the model also worked to the advantage of the measurement system, allowing the number of measurement channels to be doubled to 32 since it was possible to increase the number of JAXA in-house data recorders to four. Sixteen measurement channels were allocated to accelerometer measurements, and the remaining 16 to pressure transducer measurements.

As with the MoDKI, the free-flight aerodynamic measurement technique was applied to the aerodynamic measurement of this model [8,11]. This technique is capable of measuring multi-component forces in a very short time. During the test, the model is completely unconstrained and is not subject to aerodynamic interference from the support system (model support sting or stand), as in real flight conditions. Scramjet-integrated airframe models require all equipment to be mounted inside the model to perform all fuel injection and measurements autonomously, resulting in a lack of space inside the model and severely restricting the location of the accelerometers. One of the advantages of the free-flight aerodynamic measurement method is that it greatly reduces the constraints on accelerometer mounting locations.

## 2.2. Free-flight force measurement technique

In 2010, HUEST successfully developed a free-flight aerodynamic measurement method [12] under hypersonic flow conditions and applied it to multi-component force measurement using aerodynamic models of various shapes. This method is free-flying during the test period and, therefore, completely free from mechanical or aerodynamic interference from model support systems such as sting, wires, and stand, which are crucial for conventional force measurement techniques. Although there are requirements for using differential accelerometers and only valid within extremely short test time, piezoelectric uniaxial accelerometers, readily available and inexpensive, can be used to measure multiple forces, including rotational forces. Furthermore, this method is flexible even when the model's size restricts the accelerometers' location, making it the most suitable aerodynamic measurement method for extremely short-time tests for impulsive facilities.



**Fig 1.** (a) Schematic of the scramjet-airframe integrated model NAMaSU and (b) a picture of NAMaSU charging gaseous hydrogen.

In the NAMaSU setup, 16 uniaxial accelerometers were offset in the three orthogonal axes of the NAMaSU. Since we only focus on the three-component forces of drag, lift, and pitching moment, the 16 accelerometer measurements were processed to correspond to the dominant system.

**Table 1** Specification of NAMaSU

Length (m)	1.07
Width (m)	0.224
Height (m)	0.139
Mass (kg)	37.8
Instruments	Onboard data recorder x 4 (32 channels) Accelerometer (PCB352C65) x 16 Pressure transducer (PCB113B12) x 16
Fuel supply	Gaseous Hydrogen tank: Swagelok 304L-HDF4-300, 300mL x 2 Fast-acting valve: Circle seals SV30U2NC8P43 Timer : OMRON H3Y x 4

### 2.3. Scramjet design modification

The MoDKI scramjet design (Fig.2a) used in previous studies was based on scramjet research results from JAXA Kakuda. The main operating region of this scramjet combustion chamber was supersonic flow conditions below Mach 6, and it was unsuitable for supersonic flow, where the scramjet should originally perform. The combustion reaction is highly dependent on subsonic combustion in the recirculation region inside the combustor cavity, and the design is based on the assumption that combustion is completed in an extremely short combustor. A nozzle with a large expansion angle follows immediately after the combustor and is expected to generate thrust. The Mach number at the combustor inlet assumed in this design is about 2 at most, and fuel/air mixing and combustion completion inside the cavity are possible with a low Mach number flow of this magnitude. However, for hypersonic flows with Mach numbers of 8 or higher, combustion inside the cavity becomes difficult because the pronounced compressibility of the free stream hinders the mixing of fuel and air inside the cavity. In previous HIRST experiments, fuel and air mixing in the cavity became difficult when the inside of the combustor exceeded Mach number 4. This tendency becomes even more pronounced as the compressibility becomes predominant with increasing Mach number. Therefore, in hypersonic flows, it is essential to design the length of the combustor, i.e., the time spent inside the combustor, to be sufficient to complete the recombination reaction before the nozzle expands. Nevertheless, the length of the MoDKI combustor is not sufficient. A large nozzle expansion angle downstream of the combustor is not expected to accelerate the recombination reaction at the nozzle because the pressure and temperature downstream of the combustor drop rapidly.

In contrast to the MoDKI, the NAMaSU shown in Fig 2b has a longer combustor length and aims to ensure a longer combustion time by sufficiently preventing the pressure and temperature drop required for recombination. The required combustor length was determined based on previous research reports [13-15], assuming a free-stream static pressure of 50 kPa and a static pressure temperature of 1050 K. The NAMaSU scramjet was designed for flight equivalent Mach 11 free-stream conditions (Table 1) with a combustor inlet static temperature/static pressure of 1100 K/50 kPa (Table 2), and a three-stage compression inlet with airframe compression and cowl compression was used to achieve the target static pressure and temperature.

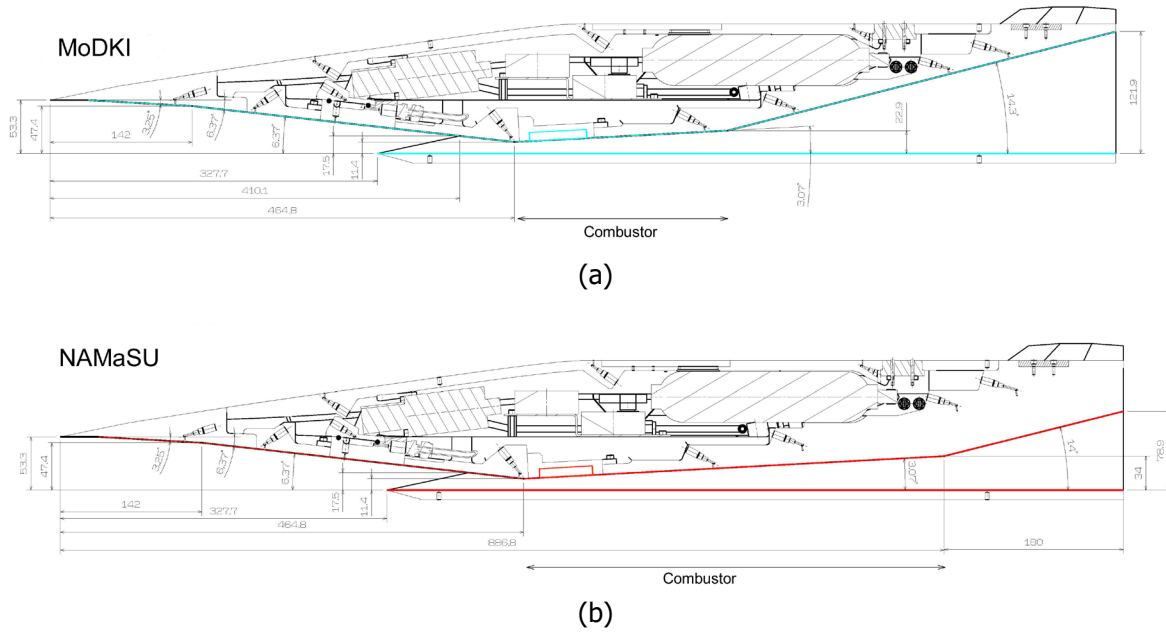


**Fig 2.** A cross-section drawing of MoDKI (a) and NAMaSU(b).

## 2.4. Hiest test condition

The NAMaSU is designed to have inlets with combustor inlet temperature pressures of 1050 K and 50 KPa (Table 2) under flight equivalent Mach number 11 conditions at Hiest, as shown in Table 3. Nominal Hiest free-stream conditions that match the inlet condition are shown in Table 3. A slower (lower enthalpy) flight equivalent Mach number of 9 was also set, which deviates from the nominal operating condition; it should be noted that the test free-stream Mach number is lower than the actual flight Mach number because of the higher static temperature of the Hiest nozzle free-stream.

**Table 2** NAMaSU Combustor entrance condition

	Mach 11 (#3142)	Mach 9 (#3128)
$p_{\infty}$ [kPa]	51	21
$T_{\infty}$ [ $\times 10^3$ K]	1.1	0.7
$M_{\infty}$	4.4	4.6

**Table 3** Hiest free-stream condition

	Mach 11 (#3142)	Mach 9 (#3128)
$p_0$ [MPa]	37	16
$T_0$ [ $\times 10^3$ K]	4.3	3.0
$H_0$ [MJ/kg]	5.8	3.7
$p_{\infty}$ [kPa]	4.0	1.4
$T_{\infty}$ [ $\times 10^2$ K]	5.2	2.8
$\rho_{\infty}$ [ $\times 10^{-2}$ kg/m <sup>3</sup> ]	2.7	1.7
$U_{\infty}$ [km/s]	3.3	2.6



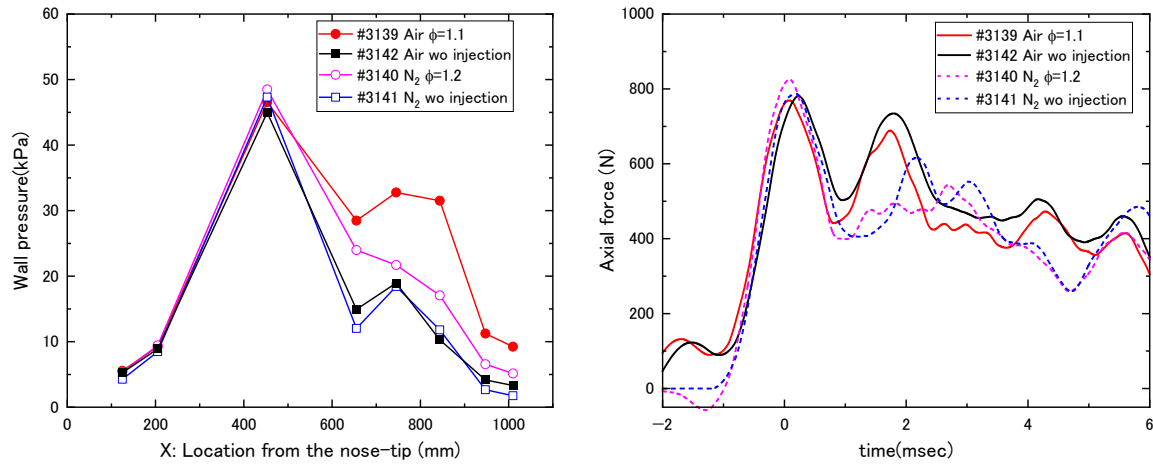
$\rho_{\infty} U_{\infty}^2 [\times 10^2 \text{ kPa}]$	2.7	2.3
$M_{\infty}$	7.1	7.6
$Re_{\infty} [\times 10^6 \text{ 1/m}]$	3.1	2.5

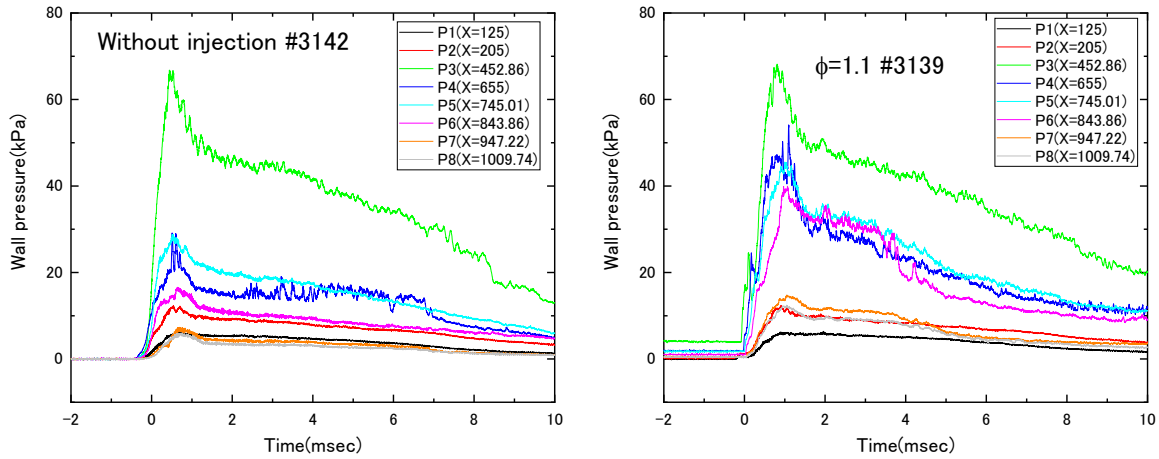
### 3. Result and discussion

Figures 3 (upper left) and (upper right) show the pressure distribution and drag history obtained at Mach number 11 (nominal design conditions). The tests were performed by varying the injection manifold pressure to a maximum hydrogen equivalence ratio of 1.1. X in the figure indicates the distance (in millimeters) from the tip of the model nose to the pressure transducer (PCB113B12). Comparing the pressure distribution of the same hydrogen mass flow (equivalent ratio 1.1) with nitrogen and air test gas, the results with air as the test gas showed a pressure increase about twice that of the nitrogen from X=700mm downstream to the nozzle, confirming that combustion is taking place inside the combustor. As is clear from the comparison between Figure 3 (lower left) and Figure 3 (lower right), combustion seems to have occurred during the period of 4 ms after the test flow arrival at the model.

However, as the drag history shows, the difference between the test results with and without hydrogen injection was small, and the thrust was not significantly increased compared to the test results with and without injection in the nitrogen test gas.

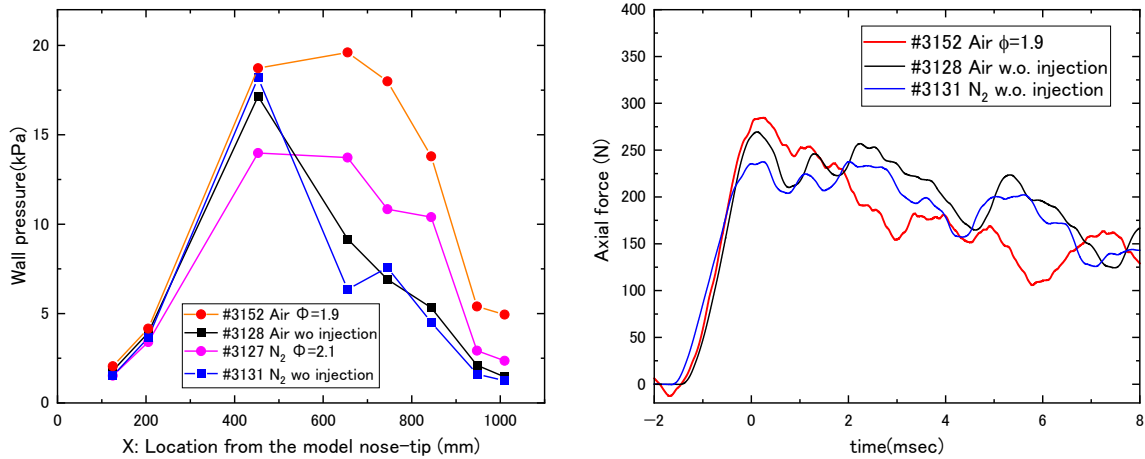
This may be because, in addition to the small pressure increase due to combustion, the test was conducted at a high Mach number 11, which corresponds to the flight speed, which increased the frictional drag of the entire fuselage, including the combustor, in addition to the decrease in specific impulse. As already pointed out in previous studies [16], the increase in frictional resistance of the combustor, along with the heat load, is a major problem for supersonic combustors and is one of the technical issues to be solved to realize scramjet because it is a trade-off with securing the combustion time (combustor length).





**Fig 3.** Results with or without gaseous hydrogen in Air or N<sub>2</sub> test gas under equivalent flight Mach number 11 ( $H_0=5.8\text{MJ/kg}$ ). Pressure distribution in the scramjet combustor (top-right) and Drag histories (top-left). Wall pressure histories without (bottom-left) or with (bottom-right) gaseous hydrogen injection. X in the figure indicates the distance (in millimeters) from the tip of the model nose to the pressure transducer (PCB113B12).

Next, tests were conducted under free-stream conditions outside the combustor's nominal operating conditions but with a lower flight equivalent Mach number of 9. The combustor inlet and Hiest data free-stream conditions under these conditions are shown in Tables 2 and 3, respectively. Under these conditions, the combustor inlet temperature is below 700 K, and the inlet pressure is about 21 kPa. Figures 4(top-left) and 4(top-right) show the obtained pressure distribution and thrust history, respectively. The pressure distribution shows a significant pressure increase due to combustion compared to the Mach 11 condition. The drag force measurement also shows an increase in the generated thrust due to increased combustion pressure, but it is insufficient compared to the model's total drag force. Figures 4 (bottom-left) and 4 (bottom-right) show the pressure histories with and without gas hydrogen injection. The pressure inside the combustor during gas hydrogen injection, i.e., combustion, shows intermittent pressure increase, indicating that the combustion is unstable due to insufficient fuel machine inlet temperature and pressure.



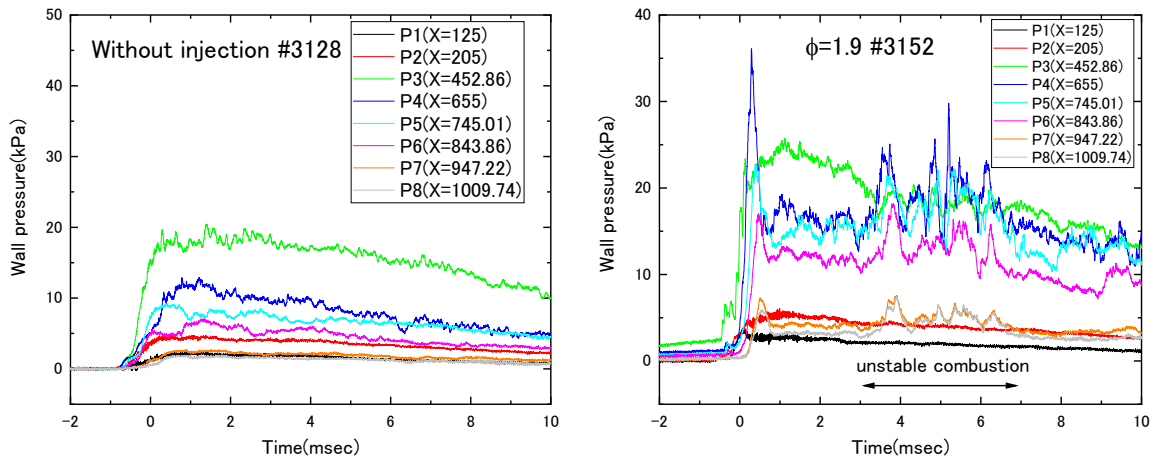


**Fig 4.** Results with or without gaseous hydrogen in Air or N<sub>2</sub> test gas under equivalent flight Mach number 9 ( $H_0=3.7\text{MJ/kg}$ ). Pressure distribution in the scramjet combustor (top-left) and Drag histories (top-right). Wall pressure histories without (bottom-left) or with (bottom-right) gaseous hydrogen injection. X in the figure indicates the distance (in millimeters) from the tip of the model nose to the pressure transducer (PCB113B12).

#### 4. Conclusion

This report presents the preliminary results of combustion tests conducted in the high-enthalpy shock tunnel HIEST on the NAMaSU, an integrated airframe and engine scramjet model. The tests were conducted using gaseous hydrogen as fuel, with the fuel equivalent ratio fixed at 1.1, and comparing air and nitrogen as the test gases to extract the effects of combustion. Combustion of gas-hydrogen fuel in air under flight-equivalent Mach 11 free-stream conditions was confirmed, and pressure increase was observed, but thrust increase was insufficient. Tests were conducted under flight-equivalent Mach 9 free-stream conditions to obtain stronger combustion pressure, which were lower than the combustor's original design conditions. Although the pressure increase due to combustion was more pronounced than under the Mach 11 conditions, the thrust increase was not greater than the drag of the entire model.

#### References

1. Stalker RJ and Morgan RG (1982) Parallel hydrogen injection into constant-area, high-enthalpy, supersonic free-stream, AIAA Journal, Vol.20, No.10, 1468-1469. <https://doi.org/10.2514/3.7987>
2. Paull A, Stalker RJ and Mee DJ (1995) Experiments on supersonic combustion ramjet propulsion in a shock tunnel. Journal of Fluid Mechanics, Volume 296, 10 August 1995, pp. 159-183. <https://doi.org/10.1017/S0022112095002096>
3. Holden M (2000) Studies of scramjet performance in the LENS facilities, 36th AIAA/ASME/SAE/ASEE Joint Propulsion Conference July 17-19, 2000, Huntsville, AIAA Paper No. 2000-3604. <https://doi.org/10.2514/6.2000-3604>
4. Itoh K, Ueda S, Tanno H, Komuro T and Sato K (2002) Hypersonic aerothermodynamic and scramjet research using high enthalpy shock tunnel. Shock Waves 12, 93-98. <https://doi.org/10.1007/s00193-002-0147-0>
5. Hannemann K, Schramm JM, Laurence SJ, Karl S, Langener T and Steelant J (2014) Experimental and numerical analysis of the small scale LAPCAT II scramjet flow path in high enthalpy shock tunnel conditions. Space Propulsion, May 19-22 2014, Cologne, Germany, SP2014-2969350.



6. Jiang Z, Zhan Z, Liu Y, Wang C and Luo C (2021) Criteria for hypersonic airbreathing propulsion and its experimental verification, Chinese Journal of Aeronautics, Volume 34, Issue 3, March 2021, Pages 94-104. <https://doi.org/10.1016/j.cja.2020.11.001>
7. Hannemann K, Schramm JM, Karl S and Laurence SJ (2015) Free flight testing of a scramjet engine in a large-scale shock tunnel. 20th AIAA International Space Planes and Hypersonic Systems and Technologies Conference, AIAA Paper No. 2015-3608. <https://doi.org/10.2514/6.2015-3608>
8. Tanno M and Tanno H (2021) Aerodynamic characteristics of a free-flight scramjet vehicle in shock tunnel. Exp Fluids 62, 150. <https://doi.org/10.1007/s00348-021-03229-0>
9. Itoh K, Ueda S, Komuro T, Sato K, Takahashi M, Miyajima H, Tanno H and Muramoto H (1998) Improvement of a free piston driver for a high-enthalpy shock tunnel, Shock Waves, volume 8, pp.215-233. <https://doi.org/10.1007/s001930050115>
10. Itoh K, Ueda S, Tanno H, Komuro T, Sato K (2002) Hypersonic aerothermodynamic and scramjet research using high enthalpy shock tunnel. Shock Waves 12, 93-98. <https://doi.org/10.1007/s00193-002-0147-0>
11. Tanno H, Komuro T, Sato K, Fujita K and Laurence SJ (2014) Free-flight measurement technique in the free-piston high-enthalpy shock tunnel. Review of Scientific Instruments, Vol.85, 045112. <https://doi.org/10.1063/1.4870920>
12. Tanno H, Sato K, Takahashi M, Itoh K and Komuro T (2010) Miniature Data-Logger for Aerodynamic Force Measurement in Impulsive Facility, AIAA Paper No. 2010-4204, The 27th AIAA Aerodynamic Measurement Technology and Ground Testing Conference, <https://doi.org/10.2514/6.2010-4204>
13. Pergament H (1963) A Theoretical Analysis of Non- -Equilibrium Hydrogen-Air reaction flow systems, AIAA Paper No.1963-113, <https://doi.org/10.2514/6.1963-113>
14. Smart MK (2010) Scramjet inlets, High Speed Propulsion: Engine Design-Integration and Thermal Management, RTO-EN-AVT-185, NATO Science and Technology Organization, Paper
15. Takahashi M, et al (2006) Effect of Combustor Shape on Scramjet Characteristics at Hypervelocity Condition over Mach 10 Flight, AIAA Paper No. 2006-8024, Published Online:15 Jun 2012 <https://doi.org/10.2514/6.2006-8024>
16. Stalker RJ, (2006) Scramjets, Sub-Orbital Flight and Skin Friction, AIAA Paper No.2006-8156, 14th International Space Planes Conference, November 2006, Canberra, <https://doi.org/10.2514/6.2006-8156>